

INTERACTIVE HYPERSONIC WAVERIDER DESIGN AND OPTIMIZATION

K. B. Center¹, K. D. Jones¹, F. C. Dougherty², A. R. Seebass³, and H. Sobieczky⁴Dept. of Aerospace Engineering Sciences, University of Colorado,
Boulder, CO 80309-0429, USAAbstract

Discussed is the development, operation, and validation of two design codes that generate waveriders based on non-axisymmetric flowfields. In the first method, an approximation is applied to generate an undersurface flowfield based on the local curvature of an arbitrary user-defined exit-plane shock shape. The code is controlled by a graphical workstation interface so that interactive modifications to the flow conditions and geometric parameters can be computed and redisplayed in real-time. The second method marches inward from a shock surface to determine the resulting waverider lower surface. The ultimate application of these codes is to serve as an expert system for the development of waveriders that are strongly competitive candidates for integration into a wide range of potential high-speed aerodynamic applications.

Nomenclature

AR	= aspect ratio
C_D	= drag coefficient, $D/(q_\infty S_{ref})$
C_L	= lift coefficient, $L/(q_\infty S_{ref})$
C_M	= moment coefficient, $P/(q_\infty S_{ref} L_{ref})$
C_V	= volume coefficient V/L_{ref}^3
D	= drag
L	= lift
L/D	= lift over drag
L_{ref}	= ref. length (symmetry-plane chord)
M_∞	= freestream Mach number
P	= pitching moment about the nose
q_∞	= freestream dynamic pressure
Re	= Reynolds number based on L_{ref}
S_{ref}	= reference area (planform area)
S_{wet}	= wetted area
T	= temperature
u, v, w, ρ, p	= primitive flow variables
X_{ac}	= streamwise aerodynamic center
X_{cent}	= streamwise centroid
V	= volume
β	= shock cone half angle
γ	= ratio of specific heats
η_v	= volumetric efficiency ($V^{2/3}/S_{wet}$)

Introduction

Over the course of the last decade, a great deal of interest has resurfaced in waveriders as viable candidates for many of the high-speed aerodynamic initiatives currently under consideration within the aerospace industry. Recent technological advancements in both materials and propulsion have brought concepts such as the National Aerospace Plane (NASP), single-stage-to-orbit vehicles, and high-speed civil transports (HSCTs) well within grasp for the early 21st century.

Although the author of the name itself is somewhat of a mystery, the term "waverider" very nicely describes the operating principle of this class of hypersonic vehicle. There are conflicting views regarding the attributes necessary to classify a vehicle as a waverider. In general, the definition states that a waverider possesses a sharp leading edge with an attached shock wave upon which the vehicle appears to ride, hence the term "waverider". This definition is acceptable if the vehicle has an infinitely sharp leading edge and is performing under truly inviscid conditions, but not when the effects of viscosity and a realistically blunt leading edge are considered. A revised and more encompassing definition is that a waverider, by virtue of its geometry, generates and contains a shock surface within the limits of the lower planform, and effectively uses the high post-shock pressure to provide the majority of the vehicle's lift.

Waveriders have traditionally been based on well defined supersonic flowfields, such as two-dimensional wedge flow¹ or conically axisymmetric flow^{2,3}. Although exact solutions are provided using these techniques, the restrictions imposed by using a portion of such simple flowfields significantly hinders the ability to design waveriders that are good candidates for integration into a realistic configuration. This can be attributed to two factors. First, basing vehicles upon purely axisymmetric or planar flowfields does not allow design of configurations that generate an arbitrary shock shape. This capability is necessary if waveriders are to be designed that will accommodate a powerplant with given inlet conditions and diffuser geometry. Secondly, the waveriders of previous stud-

¹ Grad. Res. Asst., ² Adjct. Prof., ³ Dean, College of Engineering, ⁴ Visiting Prof., permanent address: DLR, Göttingen, Germany

ies, although excellent at their design Mach number, generally perform poorly at low speeds. This difficulty arises at subsonic speeds where the aerodynamic center resides at an axial location ahead of the configuration centroid. This renders the aircraft statically unstable, an undesirable trait in any design.

Many of the shortcomings of previous studies can be overcome using non-axisymmetric shock shapes as the basis for inverse waverider design. Two methods first proposed by Sobieczky et al.⁴ are described. The first is the osculating cones method which accepts as a design condition the shape of a desired shock profile at the configuration's exit-plane. In contrast to traditional methods that are based upon simple flowfields, the osculating cones approach treats incremental stations along the effective span of the configuration as regions of locally conical flow. Using this approach permits the design of more general and practical configurations that may be better suited for a particular mission than their axisymmetric counterparts. The second method proposed by Sobieczky is a cross-stream marching procedure. The osculating cones method provides flexibility in the definition of the shock's cross-sectional shape, but requires the shock's strength to remain constant everywhere. The cross-stream marching method, on the other hand, provides flexibility in both the cross-sectional and streamwise shape of the shock allowing for the definition of truly general shock shapes. The basic cross-stream marching problem in three dimensions, however, is mathematically ill-posed, and consequently, it provides a number of rudimentary difficulties that must be overcome.

The concepts embodied by the osculating cones method have been incorporated into an interactive graphics software package that facilitates real-time manipulation of the desired shock shape, leading edge shape, upper surface topology, powerplant geometry, and governing flowfield variables, making the deduction of trends in vehicle planform and performance immediately obvious. Interactive flexibility allows substantial freedom in the rapid design of waveriders for a wide range of potential applications. Direct CFD simulations are used to validate this new class of vehicles by comparing the computationally obtained shock location, surface pressure values, and design condition aerodynamic performance, with those calculated during the interactive design session.

Cross-stream marching is the basis for a design algorithm that is currently under development

to complement the osculating cones approach, but the code is in a much earlier stage of development. Nevertheless, significant insight to the underlying theory is given, and some comparisons of preliminary results with exact solutions demonstrate the utility of the approach.

Classical Waverider Design Concept

The design of waverider configurations is inherently an inverse design problem. It is quite difficult to design a vehicle that will produce a shock wave that is attached to the leading edge at some desired cruise condition using direct methods. However, it is a relatively simple task, in theory if not in practice, to choose a desired shock wave and find the vehicle that will generate it.

The classical approach to designing "conical shock" waveriders is illustrated in fig. 1. In this approach the waverider's lower surface is "carved" out of a conical flowfield. The inviscid, supersonic flow over a slender, axisymmetric cone is described by the Taylor-Maccoll ordinary differential equation. A leading edge that lies on the conical shock wave is defined, typically, by defining a flow-capture-tube, that is, the streamwise projection of the leading edge. All of the streamlines that pass through the leading edge are used to define a streamsurface that for inviscid flow can be replaced by a solid surface. This solid surface is the waverider's lower surface, and it will generate the portion of the conical flowfield and shock wave that are contained beneath it in the absence of the slender cone used to set up the problem.

Virtually all waverider studies of the past and the present employ this approach, or slight variations, with the primary difference being the choice of the flowfield from which the waverider's lower surface is carved. Planar or conical flowfields are quite popular because exact solutions are known describing the post-shock flowfields, but the basic design approach can be applied to any generalized flowfield.

Osculating Cones Concept

Axisymmetric conical waveriders such as those investigated in the work of Bowcutt always generate shocks that are a portion of a right circular cone, therefore the shock profiles at the exit-plane of the configuration are arcs of constant radius. In contrast, osculating cones waveriders are generated by specifying a completely arbitrary shock shape at the configuration's exit-plane and treating each region along the span of the shock as a region of locally conical flow. If the curvature of this shock pro-

file is evaluated at each station along its arclength, the reciprocal is the radius of a hypothetical osculating cone (that is, a cone whose curvature exactly matches that of the shock surface at the point of tangency). A constant shock angle in each local region of osculation is enforced, therefore the streamwise location of the vertex in each osculating region is known and used as a reference origin for the Taylor-Maccoll solution. This restriction insures that any shock surface generated will be of constant strength.

Once the regions of osculation have been determined, a flow capture tube is defined by specifying an inwardly directed normal distance from the point that defines the exit-plane shock profile in each osculating region. To insure a physical solution, this normal distance must locate a point within the physical regime of the Taylor-Maccoll solution. When the (y, z) location of this point is projected forward in the direction of the freestream, it will intersect the shock surface at some axial location, defining the three-dimensional leading edge coordinates within that locally conical region. Connecting these points forms the waverider's leading edge. Figure 2 is a view of a typical osculating cones waverider exit-plane. The dashed line is the specified shock shape. Local cone radii and vertices are indicated as dotted lines and diamonds respectively. The normal distances that define the leading edge lie within the dotted regions of each local cone and are represented as squares.

Upon complete definition of the leading edge, determination of the waverider's lower surface is a simple matter of integrating a streamsurface from the leading edge to the exit-plane within the local region of osculation using the velocity components from the Taylor-Maccoll solution. The intersection of these streamlines with the configuration's exit-plane is indicated as a series of triangles in fig. 2.

Figure 3 also displays the exit plane of a waverider generated using the method of osculating cones. This configuration, however, is the degeneration of the method to an axisymmetric case. The shock shape is clearly a circular arc segment. Consequently each station along the shock profile has the same effective local cone radius and shares a common conical vertex.

Interactive Design The osculating cones approach provides a powerful basis for the design of non-traditional waverider geometries. Initial application of the method proved cumbersome, as do most purely computational codes, because of the lack of automation in the design process. An example of a typical procedure to generate a waverider would be as fol-

lows: A first guess is made to define the relevant parameters, which are read in as an input template. The code works on the input data and provides a surface data set. This data set is then viewed using a visualization tool, and only at this time can the effect of the defining parameters be assessed. Conclusions are drawn and any modifications, however minor, are made to the input template and the process is repeated iteratively until a satisfactory configuration has been obtained. A logical alternative to this lengthy procedure is the incorporation of each of these components into a workstation-based software package that performs all modifications through interactive manipulation in a graphics environment.

The resulting interface is called WIPAR (Waverider Interactive Parameter Adjustment Routine). WIPAR allows interactive manipulation of the parameters that govern the inverse design of osculating cones-based waveriders. For a given set of flight conditions, these capabilities include specification of the exit-plane shock shape, independent design of the upper and lower surfaces, powerplant integration, inclusion of viscous effects, complete on-design performance analysis, and the ability to output computational grids for the purpose of flow solver validation or experimental model fabrication.

The package was originally developed for use on a Silicon Graphics 3130 graphics workstation⁵. Operational capabilities have since been extended to run on any of the newer generation 4D series machines as well. On a reasonably fine computational surface mesh (41x61), interactive manipulation of the upper and lower surface is accomplished in real-time. On a Silicon Graphics 4D35 GT calculation of the inviscid flowfield and generation of the surface geometry takes approximately .2 seconds, while the more complex viscous analysis takes roughly 10 seconds. Of course, for preliminary work, much coarser meshes may be used, with accordingly shorter turn-around times.

Lower Surface Design The design conditions for a specific waverider mission are easy to define. The ambient conditions, freestream Mach number, M_∞ , and the ratio of specific heats, γ , need only be supplemented with a desired shock angle, β , and a user-defined exit-plane shock shape and leading edge to generate the lower surface of the configuration.

In WIPAR, all variable design conditions are modified using interactive slide controls that allow both fine and substantial control of the current value. The values of M_∞ , γ , and β are set using these slide controls. The shape of the shock is controlled by

two analytic functions (called “keys”) which define the spanwise and vertical coordinates of the shock surface at the configuration’s exit-plane. The resulting curve is referred to as the Inlet Capture Curve (ICC) because it can be used as a geometric parameter in cases where we wish to specify the shape of the powerplant inlet lip as a design condition. A third key applies an inwardly directed normal distance at each station along the ICC to define a family of (y, z) coordinates at the exit-plane. These points can be thought of as a Flow Capture Tube (FCT) that cuts through the shock surface in the streamwise direction, hence the nomenclature. When the location of these points is projected forward in the direction of the freestream, they will intersect the shock surface at some axial location, defining the x -coordinate of the leading edge within their respective conical regions. Once the points comprising the leading edge have been determined, the lower surface is completed by integrating a streamline from the leading edge to the exit-plane in each local region of osculation using the velocity components obtained in the Taylor-Maccoll solution. Values of the primitive flow variables are constant along rays intersecting the vertex of the local cone. To determine the surface values of pressure, Mach number, and the velocity components merely requires calculation of the local azimuthal angle.

Upper Surface Design While the lower surface geometry of the waverider is very tightly constrained by the need to maintain a continuous, attached, constant strength shock, the upper surface design leaves more to the discretion of the designer. A delicate balance exists between enhancing the lift-to-drag ratio provided by the lower surface as much as possible and providing enough usable internal volume to accommodate the fuel and passengers desired for the aircraft’s mission.

In WIPAR, the shape of the upper surface is governed by two keys. The first key defines an inward deviation of the upper surface from the FCT as a function of axial location. The same key is applied to every locally conical region and in each case the deviation is governed by a user-defined function that maps a displacement value to the normalized distance between the leading and trailing edges. The second key acts to scale the effect of the first key, so that the effect of upper surface closure can be controlled along the span in each region.

Determination of the primitive variable values on the upper surface requires application of an accurate but rapid computational analysis. This is

accomplished in WIPAR by use of an approximate scheme that applies the axisymmetric method of characteristics. Once the upper surface has been defined, a family of approximate streamline-oriented lines must be extracted to serve as the marching domain for application of the characteristic method. Locations are defined along the leading edge to serve as starting points. For each successive axial station, the y and z components are determined by finding the intersection of the streamwise projected upper surface with the normal of the previous projection. Figure 4a shows the streamwise projection of an osculating cones waverider. The horizontally-oriented lines are the grid lines of several axial stations. The vertically-oriented lines on the left side are the marching lines. The vertically-oriented lines on the right side of the fig. are the spanwise grid lines. The same information is contained in fig. 4b, which is displayed in perspective as a visual aid. These coordinates, along with local values of effective cylindrical radius and streamwise angular deviation are computed and stored for each axial location. Flow properties along the length of each marching line are obtained through application of the compatibility equation form of the axisymmetric method of characteristics. Using freestream velocity as the starting condition, subsequent downstream values are obtained by using the local values of effective radius, streamwise angular deviation, and axial displacement in the compatibility equations and marching via fourth-order Runge-Kutta. Once the flow variables have been obtained along all marching lines, the values are redistributed onto the original surface grid.

Viscous Considerations Viscous effects play a large role in the performance of high-speed aircraft. Consequently, these effects must be considered at the design condition if a reasonable analysis is to be performed. The growth of the boundary layer along the length of the vehicle leads to a degradation of performance both through the addition of a skin friction component to the drag and to a small extent through the separation of the bow shock from the leading edge.

Viscous effects are determined using the same streamline-oriented marching lines implemented in the upper surface method of characteristics analysis. The variables used for the boundary layer analysis (p, ρ, T, M , and u) are obtained in the inviscid analysis. Separate computational solution schemes are applied for the laminar and turbulent regimes. The transitional region is correlated to experimental

data based on local Reynolds number. The computation is initiated at the first index (corresponding to the leading edge) of each marching line. Laminar boundary layer growth is calculated using Walz' integral method⁶ which numerically solves the boundary layer momentum equation and the mechanical energy equation, a set of coupled first-order ordinary differential equations. Laminar methods are applied until a threshold local Reynolds number is reached. This is the beginning of transition. Correlation with experimental data from supersonic wings provides the boundary layer profile through the transitional regime⁷. The end of transition is predicted using an equation attributed to Harris and Blanchard⁸. Turbulent computations are initiated at the end of transition. The method of White and Christoph⁹ is an integral method which, depending on the value of skin friction coefficient, solves one of two first-order ordinary differential equations. Turbulent computations continue to the end of the configuration or until turbulent separation occurs. No effort is made to capture the effects of separated flow. Instead the analysis is halted and the user is informed of the inability to proceed.

Work in progress currently seeks to geometrically modify the surface of WIPAR waveriders to account for losses due to viscous effects. After the boundary layer thickness has been determined over the entire surface of the Euler-derived waveriders, a subtraction of this viscous layer from the original inviscid configuration may be applied to provide a waverider that more closely exhibits on-design performance when operating under viscous conditions.

Test Cases and Results The first round of validation studies for WIPAR involved an investigation into the ability of the osculating cones method to properly recover the originally specified shock profile and lower surface pressures. Using five test cases, (four Mach 4 cases and one Mach 6.0 case), surface geometries interactively designed in WIPAR were extracted and analysed using F3D, a robust NASA flow solver⁵. Each case was designed to represent conceivable difficulties in the application of the osculating cones method. The results obtained from Euler simulations showed exceptionally good agreement between both the surface pressure values and the position of the shock.

All of the initial test configurations were designed with freestream upper surfaces and truncated bases. Capabilities in WIPAR now permit the specification of arbitrary upper surfaces. To assess the accuracy of the method of characteristics approxi-

mation applied to the upper surface evaluation in WIPAR, a Mach 8 test case (shown in fig. 5) was generated and its geometry evaluated in F3D. Figures 6a, b, and c compare the values of surface pressure at an axial station 50% of the distance to the exit-plane of the waverider, a station 90% of the distance, and along the length of the symmetry plane, respectively. The solid line (WIPAR) and the dashed line (F3D) denote surface pressure values from the upper symmetry plane, around the sharp leading edge, and back to the lower symmetry plane. Although slight deviations exist over small regions of each cross-section, the net pressure differential of the configuration as determined in WIPAR and by F3D are very consistent. The inviscid lift-to-drag values obtained in WIPAR and F3D are 5.94 and 5.92 respectively.

From a design standpoint, it is desirable to generate configurations that do not have blunt bases, primarily because of the difficulty in accurately determining their aerodynamic contribution to configuration performance. At Mach numbers of 5 or less, complete closure at the exit-plane is almost always possible if the taper of the upper surface in the streamwise direction is smoothly defined and does not expand surface pressure to vacuum conditions (in which case the flow can not be predicted by the axisymmetric method of characteristics).

With the aforementioned considerations in mind, two new configurations are presented as competitive candidates for a hypothetical Mach 4 HSCT mission. Both cases have closed exit-planes, and the primary consideration during the interactive design phase was the localization of internal volume to the centerline (where it is most usable as component packaging space) while preserving as much as possible the exceptional lift-to-drag values for which waveriders are noted. Case 1 is a blunt-nosed configuration with a straight delta-wing planform. A rectangular cross-section situated at the centerline could accommodate a passenger cabin. Drooped nacelle-like features on the lower surface provide excellent containment volume for powerplant components and fuel cells. Case 2 has a sharper nose and a complex leading edge sweep to enhance low-speed aerodynamic performance characteristics. The majority of the volume is contained within a circular fuselage-like feature that can be packaged in much the same manner as more conventional configurations. Although no formal optimization code has been applied to determine these aircraft, they have been "manually optimized" in WIPAR to the satisfaction of the designer for viscous lift-to-drag ratio, practical plan-

form, and volumetric efficiency. The lower surface of Bowcutt's optimized Mach 4 conical waverider was duplicated and used as a comparison case. An expansion topology similar to the parabolically-tapered upper surface used in the original Bowcutt analysis was applied. The Bowcutt-type configuration is referred to in future text as case 3. Planform, frontal, side, and perspective views of each surface geometry are illustrated in figs. 7, 8 and 9.

The table below compares some critical aerodynamic and geometric parameters for each of the three cases described.

Table 1: WIPAR performance results.

Case	1	2	3
C_L	0.070	0.085	0.091
C_D	0.012	0.016	0.014
L/D	6.04	5.32	6.59
C_M	0.049	0.057	0.060
C_V	0.009	0.010	0.014
S_{ref}	0.427	0.356	0.495
η_v	0.046	0.055	0.057
AR	0.780	0.761	0.829
X_{ac}	0.713	0.699	0.672
X_{cent}	0.668	0.635	0.676

Inspection of the tabulated values reveals the respectable performance values of the WIPAR generated cases as they compare with the sample axisymmetric case. It should be noted that the values obtained for case 3 compare reasonably well with the original Bowcutt optimum Mach 4 analysis. The most notable performance aspect is the static margin ($X_{ac} - X_{cent}$), which reflects the degree of static stability that each case delivers. Cases 1 and 2 both have positive values of static margin and consequently are stable configurations. Case three has slightly negative static margin and a sufficiently large moment coefficient to render the configuration statically unstable. η_v in this study is defined based on wetted area, contrary to previous studies which have used planform area as the basis. Higher values of η_v generally correspond to more efficient viscous optimized waveriders. By definition .207 is the maximum possible value of η_v , which is a sphere. This parameter is primarily an indication of the viscous contribution to the degradation of L/D . With this in mind, it is obvious that cases 1 and 2 are competitive with case 3 in reducing the effects of viscous drag penalty.

WIPAR is unique in that it allows the designer to exercise a high degree of intuition and personal expertise in the design of a configuration for a conceptual mission. The interactive nature of the package helps the user determine trends in performance, especially those dependent upon configuration geometry. In its final form WIPAR will be a complete expert system specifically structured to yield insight as to what areas of waverider design require more rigorous and comprehensive future studies.

Cross-stream Marching Concept

A second method for the design of waveriders from arbitrary shock shapes is also under development. This program is called SCIEMAP (Supersonic Cross-stream Inverse Euler Marching Program). Due to its premature state of development only a brief summary of the underlying principles of SCIEMAP is presented here. As previously mentioned, the cross-stream marching concept provides flexibility in the cross-sectional shape of the shock wave, as with the osculating cones method, but it also provides flexibility in the streamwise shape of the shock, that is, the shock's strength is allowed to vary from point to point. The definition of the post-shock flowfield is no longer a simple task. There are no exact solutions defining the flowfield, and consequently, the Euler equations must be integrated away from the shock surface in a cross-stream fashion as illustrated in fig. 10.

Ill-posedness For the steady, supersonic flows of this study the governing equations (conservation of mass, momentum, and entropy) are hyperbolic in nature. As a result of the hyperbolic form the three-dimensional problem is fundamentally ill-posed, that is, the problem may not be continuously dependent on the initial data, or in simpler terms, the wrong boundary conditions are given for the set of governing equations. The cause of the ill-posedness can be seen graphically in fig. 11. In three dimensions the characteristics are conoids, as illustrated, with well defined domains of dependence and influence. Intuitively, data from outside these conoids should not be used to influence point P . Unfortunately, this is precisely what must be done for this problem.

The effects of the problem's ill-posedness can be seen mathematically by considering a simple model equation

$$\phi_{xx} - \phi_{yy} - \phi_{zz} = 0. \quad (1)$$

The solution to eqn. 1 is

$$\phi = \exp(ik_1x + ik_2y + ik_3z) \quad (2)$$

where $i = \sqrt{-1}$. By substitution it can be seen that

$$k_3 = \pm \sqrt{k_1^2 - k_2^2}. \quad (3)$$

Hence, if the wavenumber in the y -direction is greater than the wavenumber in the x -direction, the solution will grow exponentially in the z -direction. However, a similar problem in two dimensions is well-posed for marching in either a streamwise or a cross-stream direction. Hence, the ill-posedness can be eliminated if the problem can be reduced to a two-dimensional one.

Marching Approach To obtain a well-posed problem the governing equations must be transformed into a coordinate system where the three-dimensional problem can be reduced to a series of two-dimensional problems. For the general case this is not possible, but the proper choice of coordinate systems can minimize the three-dimensionality, hence, minimizing the effects of the ill-posedness.

The plane in which the local flowfield most closely resembles two-dimensional flow is called the local osculating plane. The osculating plane is tangent to the streamline passing through a point and contains the principle normal to the particle's path there. Marching within the osculating plane eliminates one velocity component, since the velocity vector is contained in the osculating plane. The orientation of the local osculating plane is solution dependent, hence, the marching grid must be developed simultaneously as the solution is computed.

Preliminary Results Several simple test cases with exact solutions exist that may be used to validate the SCIEMAP algorithm. The simplest case is, of course, the two-dimensional flow over a wedge. This is not a very interesting test case, however, as all of the gradients go to zero. A more interesting case is the axisymmetric flow over a slender cone. A comparison of nondimensional pressure along a line normal to the shock surface as determined by SCIEMAP and the Taylor-Maccoll solution is shown in fig. 12. The shock angle is approximately 26° with a freestream Mach number of 4 and a specific heat ratio of 1.4. The SCIEMAP solution contains only 10 grid points in the marched direction, and as can be seen the two methods are in excellent agreement for such a coarse grid.

The cross-stream marching procedure employed in SCIEMAP offers increased flexibility over other methods in the selection of waverider shock shapes, and it provides a higher degree of accuracy than the osculating cones approach of WIPAR. The algorithm is, unfortunately, much more computationally expensive making it less desirable for use in interactive and optimization applications. Coupled with the WIPAR routine, however, the pair should provide a formidable tool for the design of waverider configurations, using SCIEMAP to refine and further optimize the output of WIPAR.

Conclusions

The driving force behind the continuing development of the WIPAR and SCIEMAP design tools is the ability to generate efficient and practical waveriders from arbitrary shock shapes.

WIPAR currently provides the ability to specify an exit-plane shock profile, leading edge shape, and arbitrary upper surface topology that constitute a waverider configuration customized to a specific high-speed application. Cases 1 and 2 are excellent preliminary examples of the types of aircraft that can be generated using this interactive design tool. Results from the performance analysis of these configurations demonstrate great promise for the osculating cones design concept as a means of generating geometrically practical waveriders very rapidly. Although the lift-to-drag values of the test configurations are extremely respectable, it is important to note that they have not been optimized. Future efforts will concentrate on the development of optimization strategies that will make the subtle changes necessary to provide the maximum possible performance enhancement to a preliminary configuration within geometric constraints imposed by the designer.

SCIEMAP will eventually complement WIPAR by applying a more rigorous evaluation of the waveriders designed in WIPAR and exploring shock surfaces of complex curvature that cannot be assessed using the osculating cones approximation.

In final form, these design tools will be integrated into an expert system for the rigorous design and optimization of practical waveriders for missions as diverse as high-speed civil transports and single-stage-to-orbit vehicles. The inherent flexibility of designing to an arbitrarily specified shock provides the power to design more geometrically feasible waveriders. Inverse strategies applied in both the osculating cones approximation and the cross-stream

marching approach facilitate rapid generation of surface geometries based on the design parameters. In addition, the interactive user interface provided by WIPAR is invaluable as a link between the pure performance of a conceptual aircraft and the designer's sense of geometric practicality. In combination these elements will serve as a guide in the refinement of current hypersonic concepts and the development of future high-speed aerodynamic concepts.

References

¹ Nonweiler, T. R. F., "Aerodynamic Problems of Manned Space Vehicles," *Journal of the Royal Aeronautical Society*, Vol. 63, 1959, pp. 521-528.

² Jones, J. G., "A Method for Designing Lifting Configurations for High Supersonic Speeds Using the Flow Fields of Non-Lifting Cones," Royal Aircraft Establishment, Report No. Aero. 2674, March 1963.

³ Bowcutt, K. G., Anderson, J. D., and Capriotti, D., "Viscous Optimized Hypersonic Waveriders," AIAA Paper 87-0272, January, 1987.

⁴ Sobieczky, H., Dougherty, F. C., and Jones, K. D., "Hypersonic Waverider Design for Given Shock Waves," Proceedings of the *1st International Waverider Symposium*, University of Maryland, Oct. 17-19, 1990.

⁵ Center, K.B., Sobieczky, H., and Dougherty, F. C., "Interactive Design of Hypersonic Waverider Geometries," AIAA Paper No. 91-1697, June 1991.

⁶ Walz, A., "Boundary Layers of Flow and Temperature", M.I.T. Press, Cambridge, Mass., 1969.

⁷ Pate, S.R., and Groth, E.E., "Boundary-Layer Transition Measurements on Swept Wings with Supersonic Leading Edges," *AIAA Journal*, Vol. 4, No. 4, April 1966, pp. 737-738.

⁸ DeJarnette, F.R., Kania, L.A., Chitty, A., "Aero-dynamic Heating and Surface Temperature on Vehicles for Computer - Aided Design Design Studies," AIAA-83-0411, Jan. 1983.

⁹ White, F.M., Viscous Fluid Flow, McGraw-Hill, New York, 1974, pp. 653-657.

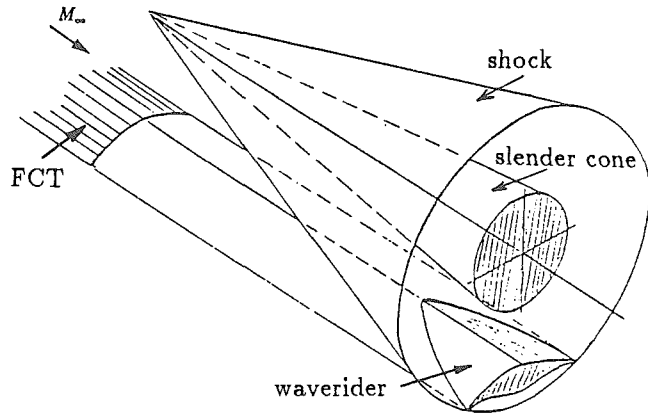


Figure 1: Classical waverider design concept for conical flow.

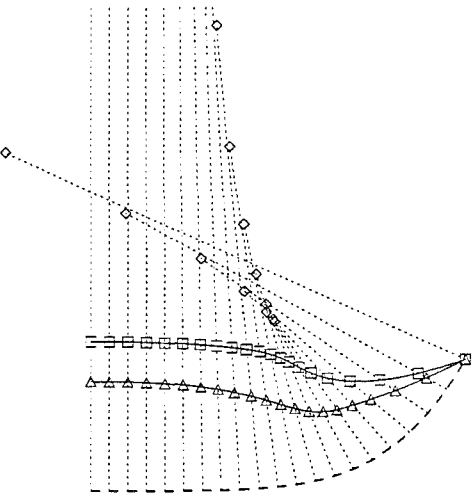


Figure 2: Schematic of osculating cones waverider exit-plane demonstrating key features of the method.

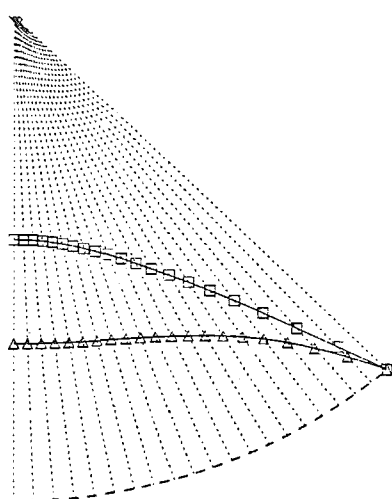


Figure 3: Schematic of degenerative osculating cones case representing an axisymmetric conical waverider.

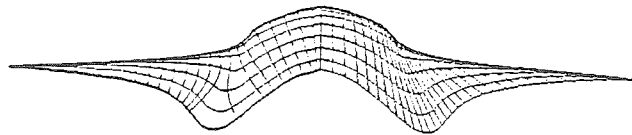


Figure 4a: Streamwise projection of a WIPAR waverider showing marching lines on the left and surface mesh on the right.

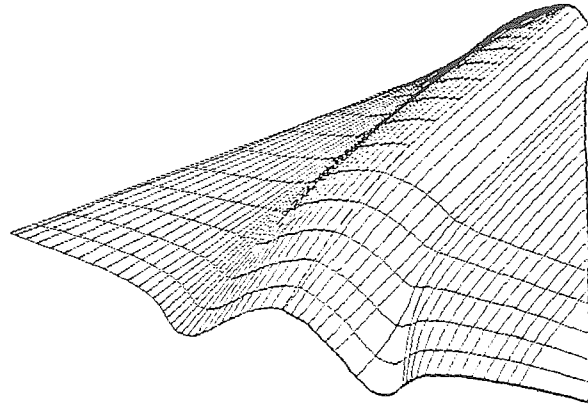


Figure 4b: Perspective view of the same configuration.

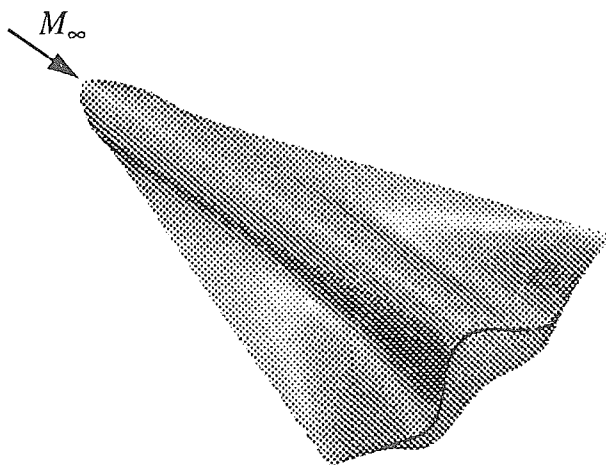


Figure 5: Perspective view of a WIPAR Mach 8 test configuration for surface pressure validation.

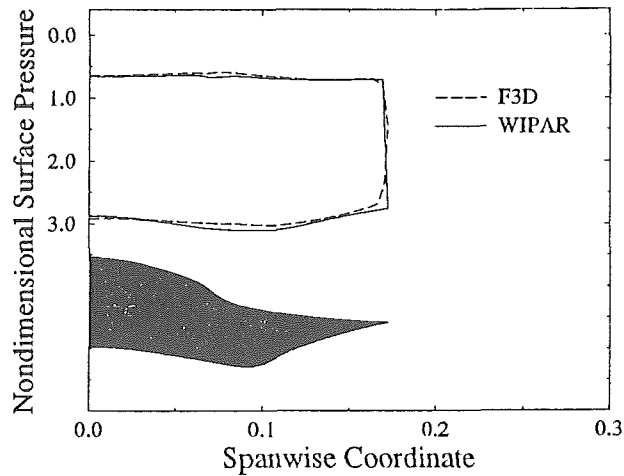


Figure 6a: Comparison of WIPAR and F3D surface pressures at the 50% streamwise station.

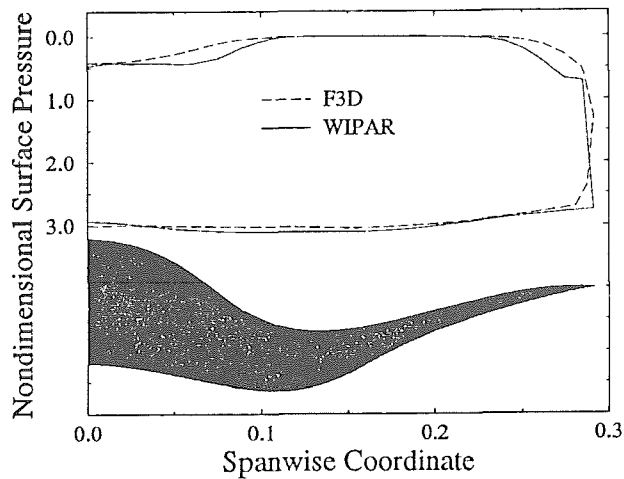


Figure 6b: Comparison of WIPAR and F3D surface pressures at the 90% streamwise station.

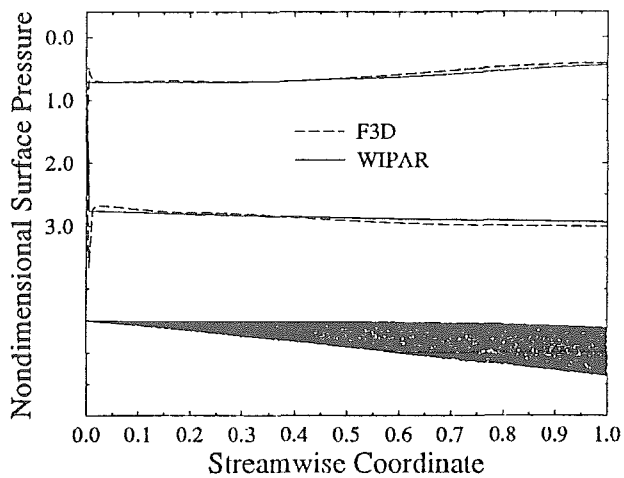


Figure 6c: Comparison of WIPAR and F3D surface pressures along the symmetry plane.

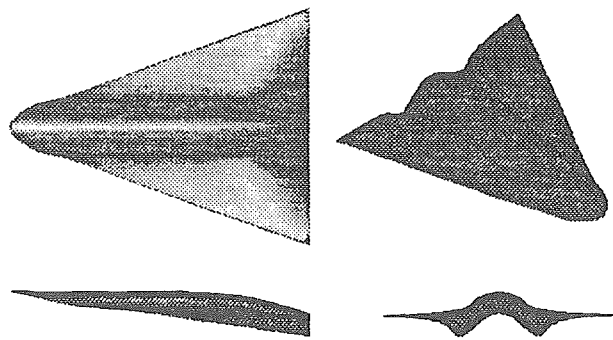


Figure 7: Planform, frontal, side, and perspective views of case 1.

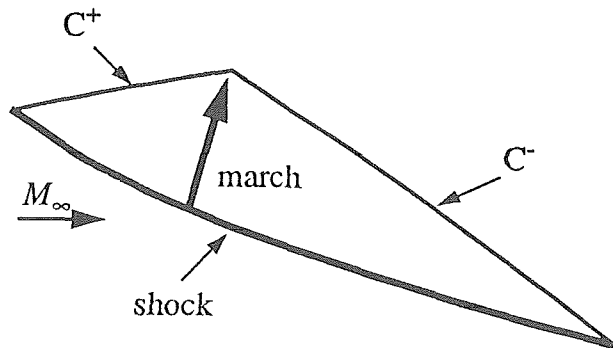


Figure 10: Cross-stream marching schematic.

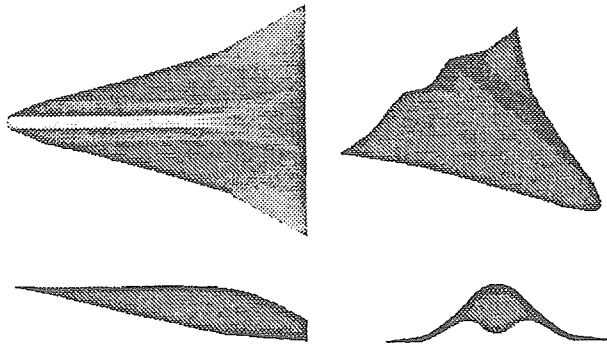


Figure 8: Planform, frontal, side, and perspective views of case 2.

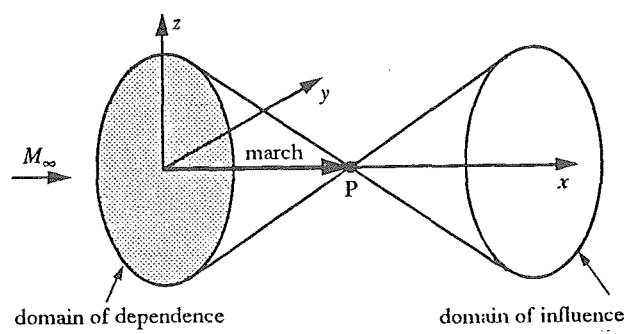


Figure 11: Characteristic conoids of the 3-D, hyperbolic model equation.

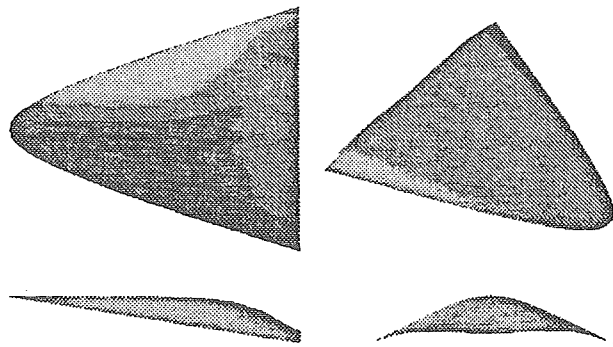


Figure 9: Planform, frontal, side, and perspective views of case 3.

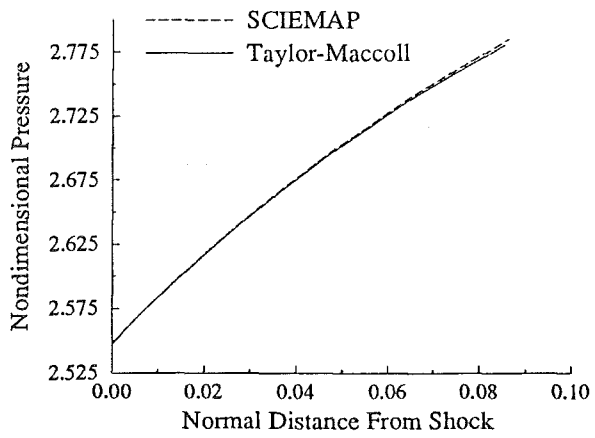


Figure 12: Axisymmetric cone flow. Comparison of nondimensional pressures computed by SCIMAP and the Taylor-Maccoll equation.